A MATHEMATICAL FUNCTION FOR DESCRIBING THE DEPENDENCE OF THE MASS ATTENUATION COEFFICIENT VERSUS ENERGY FOR COMPOSITE MATERIALS IN AN ENERGY RANGE OF 100 keV TO 2 MeV

by

Nguyen Ti Kim ANH, Lam Duj NHAT, Ho Ti Tujet NGAN, and Hoang Due TAM*

Department of Nuclear Physics, Faculty of Physics,
Ho Chi Minh City University of Education, Ho Chi Minh City, Vietnam

Scientific paper
https://doi.org/10.2298/NTRP180621001A

This work proposes a mathematical function for describing the dependence of mass attenuation coefficients *vs*. energy for composite materials in the range of 100 keV to 2 MeV. The obtained results show that the proposed function is capable of accurately describing the data with a coefficient of determination of approximately 1 for all investigated materials. Using the proposed mathematical function, the mass attenuation coefficients were interpolated and compared with the results from the Monte Carlo simulation. The results show good agreement when the simulated to interpolated mass attenuation coefficient ratios are in the range from 0.95 to 1.05. Moreover, the values of interpolated mass attenuation coefficients have also been compared with the experimental data in the previous works which indicates that most of these ratios range from 0.9 to 1.1.

Key words: mass attenuation, Monte Carlo simulation, fitting function, composite material

INTRODUCTION

Gamma radiation is widely applied in many fields such as industry [1-3], agriculture [4, 5] and medicine [6-8]. Since a gamma-ray has high energy and can easily penetrate into matter, it is used in many applications, especially structural investigations of material [9-11], testing tube defects [12, 13], determining material thickness [1], and determining liquid density [14]. However, the widespread use of a radioactive source brings hidden hazards to human health. Recent works on radiation shielding found new materials for reducing radiation hazards. These works focus on investigating the attenuation properties of various types of composite materials such as glass material groups, including PbO-BaO-B_2O_3 glass systems [15], gadolinium-based oxide and oxyfluoride glass systems [16], borate-tellurite-silicate glass systems [17]; the mixture material group, including Portland cement [18], cement and concrete [19], granite [20], and the polymer material group, including Kapton and polymethyl methacrylate (PMMA) [21]. Previous works have examined the shielding properties of composite materials for only certain energies, therefore studying the change of shielding properties in a wide range of gamma-ray energy is very necessary.

The mass attenuation coefficient (MAC) is the most important parameter for evaluating the shielding properties of materials. This parameter depends not only on the composition of material, it also depends on radiation energy. The works related to these problems were performed. However, proposing a mathematical function, for describing the dependence of MAC *vs*. energy for composite materials in a certain energy range, has not been considered in the previous works.

In this work, a mathematical function was proposed which is appropriate to describe the change of MAC *vs*. energy for composite materials in the energy range from 100 keV to 2 MeV. For energies under 100 keV, it is very difficult to find a function for describing the energy dependence of MAC due to the absorption edges from constituent elements. In fact, the energy range of 100 keV to 2 MeV is large enough to cover the energies emitted from common isotope sources in the environment. Moreover, gamma-ray sources having energy ranging from 100 keV to 2 MeV are widely used in radiography, density and thickness gauges. Therefore, it is reasonable to study the attenuation feature of materials in this energy range.

For studies on radiation shielding properties of composite materials, it is extremely useful and significant to have a mathematical function which describes the change of MAC *vs*. energy. And more importantly, it allows quick and accurate calculations of MAC at concerned energies using the interpolated method.

The reliability of the proposed function was evaluated via coefficients of determination, R^2, and in-

* Corresponding author; e-mail: hoangductam@hcmup.edu.vn

terpolated the MAC corresponding to various energies. The comparative results between the interpolated MAC, the simulated MAC and the experimental data were used as the basis for validating the proposed function.

MATERIALS AND COMPUTATIONAL METHOD

Materials

The composite materials used in the present works were divided into two groups. The first group includes the composite materials in which MAC decreases sharply with the increase of energy (group A). This group includes PbO-BaO -B_2O_3 glass systems [15], gadolinium-based oxide and oxyfluoride glass systems [16], and borate-tellurite-silicate glass systems [17]. The second group includes the mixture and polymer materials in which MAC decreases steadily with the increase of energy (group B). This group includes Portland cement [18], cement and concrete [19], granite [20], Kapton and PMMA [21]. The chemical composition and density of these materials were presented in tabs. 1 and 2. The effective atomic number of the materials are in the range from 3 to 23. With a total of 30 samples, the obtained data is reliable enough for evaluating the suitability of the fitting function.

Theoretical background

When a narrow beam of gamma rays passes through matter, its intensity is attenuated according to the Lambert-Beer law. Mathematically, the intensity of the transmitted photon beam is defined as follows

$$I(x) \quad I_0 e^{\ (\mu/\rho)\rho x} \tag{1}$$

where I_0 and I are the intensities of the incident and transmitted photon beam, respectively, (μ/ρ) is the MAC, and ρ and x are the density and thickness of target, respectively.

From eq. (1), the MAC can be rewritten

$$(\mu/\rho) \quad \frac{1}{\rho x} \ln \frac{I_0}{I} \tag{2}$$

To determine the MAC, the ratio I_0/I is required. It is important that the intensity I of the photon beam transmitted through matter without interacting is obligatory. The spectrum recorded by the detector should be the attenuated spectrum of the transmitted photon beam (known as primary photons). Any contribution of secondary photons to the recorded spectrum will decrease the accuracy of results. The common solution for limiting the contribution of the secondary photons is to use a detector collimator of a small inner diameter. Another solution used in our previous works is the advanced spectrum analysis technique [1]. By using this technique, the secondary component was considerably removed from the obtained spectra.

A mathematical function of the mass attenuation coefficient *vs.* energy

In this work, we propose a mathematical function for fitting the MAC corresponding to various energies for composite materials. This function (known as the Generalized Hyperbola function) is defined as follows

$$(\mu/\rho) \quad a \quad \frac{b}{(1 \quad cE)^{1/d}} \tag{3}$$

Table 1. Chemical composition of composite materials of group A (materials with MAC decrease sharply with the increase of energy)

	Chemical	PbO-BaO-B_2O_3 glass system (xPbO-(50-x)BaO-50B_2O_3) [15] (weight %)									Gadolinium-based oxide and oxyfluoride glass systems [16] (weight %)		Borate-tellurite-silicate glass system (xBi_2O_3-(80-x)B_2O_3-5TeO_2-15SiO_2) [17] (weight %)					
Referred code		P1	P2	P3	P4	P5	P6	P7	P8	P9	L1	L2	B1	B2	B3	B4	B5	B6
	PbO	5	10	15	20	25	30	35	40	45	–	–	–	–	–	–	–	–
	BaO	45	40	35	30	25	20	15	10	5	–	–	–	–	–	–	–	–
	B_2O_3	50	50	50	50	50	50	50	50	50	45	45	30	25	20	15	10	5
	Li_2O	–	–	–	–	–	–	–	–	–	30	30	–	–	–	–	–	–
	SrO	–	–	–	–	–	–	–	–	–	10	10	–	–	–	–	–	–
	Gd_2O_3	–	–	–	–	–	–	–	–	–	15	–	–	–	–	–	–	–
	GdF_3	–	–	–	–	–	–	–	–	–	–	15	–	–	–	–	–	–
	Bi_2O_3	–	–	–	–	–	–	–	–	–	–	–	50	55	60	65	70	75
	TeO_2	–	–	–	–	–	–	–	–	–	–	–	5	5	5	5	5	5
	SiO_3	–	–	–	–	–	–	–	–	–	–	–	15	15	15	15	15	15
Density [gcm^{-3}]		4.318	4.460	4.602	4.744	4.886	5.028	5.17	5.312	5.454	3.27	3.03	4.98	5.09	5.19	5.31	5.56	5.77

Table 2. Chemical composition of composite materials of group B (materials with MAC decrease steadily with the increase of energy)

	Chemical	Granite [20] (weight %)								Chemical	Portland cement [18] (weight %)	Element	Cement [19] (weight %)	Concrete [19] (weight %)	Kapton [21] $(C_{22}H_{10}N_2O_4)_n$ (weight %)	PMMA [21] $(C_5O_2H_8)_n$ (weight %)
Referred code		G1	G2	G3	G4	G5	G6	G7	G8		Ce1		Ce2	Ce3	Po1	Po2
	SiO_2	79.92	73.87	77.21	76.41	77.52	79.29	78.47	77.33	F	0.2807	H	–	0.9	2.6362	8
	Al_2O_3	15.99	14.79	15.45	15.3	15.52	15.87	15.71	15.48	Na_2O	0.7298	C	–	0.2	69.1133	60
	K_2O	3.24	6.24	3.34	3.83	2.79	3.01	2.06	2.69	Al_2O_3	3.8535	O	37.0	53.6	20.9235	32
	CaO	0.28	2.07	2.13	2.41	2.15	1.56	1.99	2.07	SiO_2	5.9856	N	–	–	7.3270	–
	FeO	0.24	1.36	0.86	0.91	0.94	0.01	0.81	1.09	P_2O_5	23.0198	Na	–	0.5	–	–
	Fe_2O_3	0.17	0.98	0.63	0.66	0.69	0.01	0.59	0.80	SO_3	0.1052	Mg	0.4	0.2	–	–
	TiO_2	0.06	0.20	0.17	0.21	0.18	0.12	0.12	0.27	Cl	4.6588	Al	20.9	1.3	–	–
	–	–	–	–	–	–	–	–	–	K_2O	0.0226	Si	2.1	36.7	–	–
	–	–	–	–	–	–	–	–	–	CaO	1.0155	S	–	0.1	–	–
	–	–	–	–	–	–	–	–	–	TiO_2	55.2113	K	–	0.3	–	–
	–	–	–	–	–	–	–	–	–	Cr_2O_3	0.3903	Ca	27.9	5.6	–	–
	–	–	–	–	–	–	–	–	–	MnO	0.0446	Fe	11.7	0.6	–	–
	–	–	–	–	–	–	–	–	–	Fe_2O_3	0.0974	–	–	–	–	–
	–	–	–	–	–	–	–	–	–	NiO	0.0330	–	–	–	–	–
	–	–	–	–	–	–	–	–	–	ZnO	0.0060	–	–	–	–	–
	–	–	–	–	–	–	–	–	–	Rb_2O	0.0036	–	–	–	–	–
	–	–	–	–	–	–	–	–	–	SrO	0.1541	–	–	–	–	–
	–	–	–	–	–	–	–	–	–	As_2O_3	0.0043	–	–	–	–	–
	–	–	–	–	–	–	–	–	–	BaO	0.0688	–	–	–	–	–
	–	–	–	–	–	–	–	–	–	V_2O_5	0.03048	–	–	–	–	–
Density [gcm^{-3}]		2.62	2.67	2.66	2.66	2.65	2.62	2.64	2.71		2.067		1.28	2.25	1.42	1.19

where a [cm^2g^{-1}], b [cm^2g^{-1}], c [keV^{-1}], and d are the parameters obtained by fitting eq.(3) with the MAC, corresponding to various energies, and E is the energy of gamma-ray photons.

The validation of the fitting function is based on the R^2 value. Normally, this parameter is used to evaluate the agreement of the fitting function with the data. However, the R^2 parameter shows how close the data is to the fitted curve. A high value of R^2 is not enough for stating whether the fitting function is totally suitable. Hence, the obtained fitting function was used to interpolate the MAC at various energies and used to compare the Monte Carlo simulated results and experimental data. This comparative data is the basis for validating the proposed function.

The Monte Carlo simulation

The Monte Carlo simulation using the MCNP5 code [22] was used to calculate the MAC with the aim of validating the interpolated results obtained from the fitting function. The MCNP5 code allows the building of the simulation model to be familiar with the real model of experimental arrangement. Using the available library of the MCNP5 code, we can simulate the interaction of the photon beam with matter. The obtained spectrum is the pulse height spectrum (PHS) when using Tally F8 in the MCNP5 code. From the obtained PHS, we can calculate the intensity of the photon beam before and after going through matter. From this, we can calculate the MAC at various energies.

The parameters declared in the input file of the MCNP5 code include parameters of source, parameters of the measured material and specifications of the detector. These blocks are described in detail in fig. 1. The specifications of the NaI(Tl) scintillation detector used in this work were validated in our previous works [23, 24].

The obtained PHS from the simulation is in the form of a histogram. To obtain the spectrum in the form of Gauss, we apply the FT8 GEB card in the MCNP code by using the FWHM (full width at half maximum) function. Mathematically, FWHM is defined as follows

$$\text{FWHM} \quad a \quad b\sqrt{E \quad cE^2} \tag{4}$$

where a = –0.0137257 MeV, b = 0.0739501 $MeV^{1/2}$, c = = –0.152982 MeV^{-1} [1] are the parameters, which were obtained by fitting eq. (4) with the experimental FWHM data. Depending on the type of materials, simulations run with 10^9 or 2 10^9 source particles and the relative error of simulation was kept below 0.5 %.

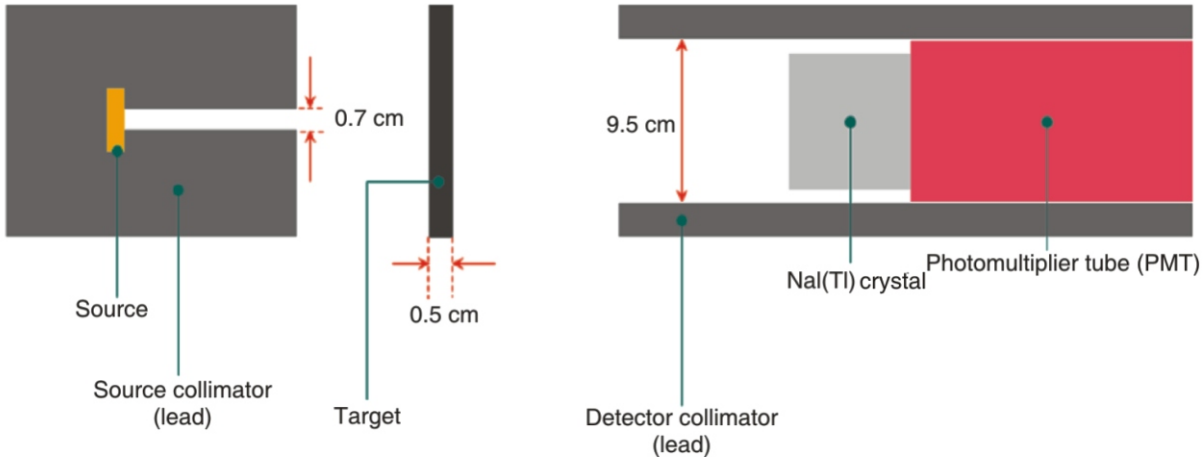

Figure 1. Schematic diagram of the cross-sectional view of the arrangement in the Monte Carlo simulation for determining the MAC

Spectrum analysis method

The inner diameter of the detector collimator was enlarged greater than usual (up to 9.5 cm). This increases the accumulated counts when using the low-strength source in the experimental measurement. Additionally, the detector collimator of a larger inner diameter will reduces the measuring time. This is very important for the NaI(Tl) detector because of its instability to change in environmental temperature during operation [25]. Enlarging the detector collimator will increase the contribution of secondary photons and hence decreases accuracy of the calculated results when using the Lambert-Beer equation. To overcome this problem, we have applied the advanced spectrum analysis technique [1] to eliminate the secondary events.

This technique consists of using the Gauss function

$$G(x) \quad \frac{A}{\sigma\sqrt{2\pi}} \exp \quad \frac{(x \quad x_0)^2}{2\sigma^2} \tag{5}$$

and 4th order polynomial function

$$\text{poly}(x) \quad a_0 \quad a_1(x \quad x_0) \quad a_2(x \quad x_0)^2 \quad a_3(x \quad x_0)^3 \quad a_4(x \quad x_0)^4 \tag{6}$$

The simulated spectra were analyzed by using Colegram software [26]. The spectrum analysis procedure is presented in fig. 2.

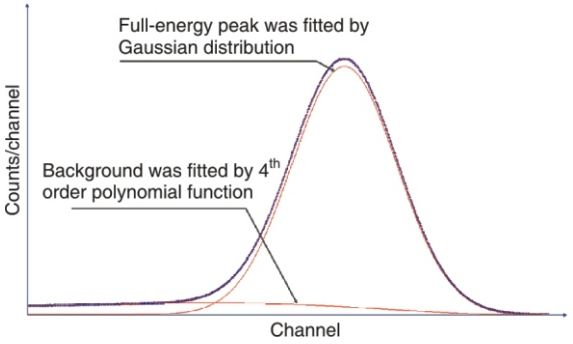

Figure 2. The spectrum analysis procedure

RESULTS AND DISCUSSION

This work aimed to find the most suitble function for describing the energy dependence of MAC for composite materials in the energy range of 100 keV to 2 MeV. The data of MAC at various energies was obtained by NIST [27]. The obtained results were presented in tab. 3. This data was fitted with eq. (3) by using the ORIGIN software. The obtained results are presented in tab. 4.

The results as shown in tab. 4 indicate that the proposed fitting function is perfectly suitable when the coefficient of determination, R^2, is approximately 1 for most of the investigated materials. For a more careful evaluation of the fitting function, the data given in tab. 4 was used to interpolate the MAC at certain energies. The obtained results were compared with the calculated results from the Monte Carlo simulation (see tab. 5) and experimental data in previous works.

Figs. 3(a)-3(f) show the change of MAC *vs*. energies for composite materials of group B. It is shown that the MAC decrease steadily with the increase of energy. Figure 4 reveals that the most simulated to interpolated MAC ratios $[(\mu/\rho)_{sim}/(\mu/\rho)_{int}]$ of materials of group B mostly range from 0.95 to 1.05. Especially for polymer materials consisting of Kapton and PMMA, this ratio only ranges from 0.96 to 1.03 (the maximum relative deviation between simulated and interpolated results of 4.3 %). These obtained results once again confirm that the proposed mathematical function is totally suitable.

The simulated to interpolated MAC ratios change with materials in group A in a wider range which is mainly from 0.9 to 1.1 (see fig. 5). For this group, the MAC decrease sharply with the increase of energy and after that they are nearly unchanged, see figs. 6(a)-6(c). Previous experience shows that inter-

Table 3. The MAC at various energies obtained from NIST [27]

	E [keV]	122	145	279	320	391	511	662	835	1115	1173	1275	1332	1408	1836
		MAC [cm^2g^{-1}]													
Group A															
$PbO-BaO-B_2O_3$ glass system	P1	0.7624	0.5182	0.1668	0.1416	0.1157	0.0930	0.0780	0.0678	0.0573	0.0557	0.0532	0.0520	0.0505	0.0443
	P2	0.8597	0.5816	0.1789	0.1502	0.1209	0.0958	0.0795	0.0686	0.0578	0.0561	0.0536	0.0523	0.0508	0.0445
	P3	0.9570	0.6450	0.1910	0.1588	0.1262	0.0985	0.0810	0.0695	0.0582	0.0566	0.0539	0.0527	0.0511	0.0448
	P4	1.0540	0.7084	0.2031	0.1673	0.1314	0.1013	0.0826	0.0704	0.0587	0.0570	0.0543	0.0530	0.0514	0.0450
	P5	1.1520	0.7718	0.2151	0.1759	0.1366	0.1040	0.0841	0.0713	0.0592	0.0574	0.0547	0.0533	0.0517	0.0453
	P6	1.2490	0.8352	0.2272	0.1845	0.1419	0.1068	0.0856	0.0722	0.0596	0.0578	0.0550	0.0537	0.0520	0.0455
	P7	1.3460	0.8986	0.2393	0.1931	0.1471	0.1095	0.0871	0.0731	0.0601	0.0582	0.0554	0.0540	0.0523	0.0458
	P8	1.4440	0.9620	0.2514	0.2016	0.1524	0.1123	0.0886	0.0740	0.0606	0.0587	0.0557	0.0543	0.0519	0.0460
	P9	1.5410	1.0250	0.2634	0.2102	0.1576	0.1151	0.0901	0.0749	0.0611	0.0591	0.0561	0.0546	0.0522	0.0462
Gadolinium- based oxide and oxyfluoride glass systems	L1	0.3948	0.2898	0.1302	0.1168	0.1018	0.0869	0.0755	0.0670	0.0575	0.0560	0.0536	0.0524	0.0509	0.0445
	L2	0.3603	0.2683	0.1266	0.1143	0.1004	0.0862	0.0752	0.0668	0.0575	0.0560	0.0536	0.0524	0.0509	0.0445
Borate-tellurite-silicate glass system	B1	1.6040	1.0590	0.2639	0.2095	0.1559	0.1138	0.0892	0.0742	0.0607	0.0587	0.0558	0.0544	0.0527	0.0463
	B2	1.7470	1.1490	0.2793	0.2201	0.1620	0.1167	0.0905	0.0749	0.0609	0.0589	0.0559	0.0545	0.0536	0.0464
	B3	1.8900	1.2400	0.2947	0.2307	0.1681	0.1196	0.0919	0.0755	0.0611	0.0590	0.0560	0.0545	0.0529	0.0465
	B4	2.0330	1.3310	0.3102	0.2413	0.1742	0.1225	0.0933	0.0762	0.0612	0.0592	0.0561	0.0546	0.0529	0.0466
	B5	2.1770	1.4210	0.3256	0.2519	0.1803	0.1254	0.0946	0.0768	0.0614	0.0593	0.0562	0.0547	0.0530	0.0466
	B6	2.3200	1.5120	0.3410	0.2626	0.1864	0.1283	0.0960	0.0774	0.0616	0.0594	0.0563	0.0547	0.0530	0.0467
Group B															
Granite	G1	0.1536	0.1423	0.1103	0.1045	0.0965	0.0863	0.0770	0.0692	0.0601	0.0586	0.0562	0.0549	0.0534	0.0466
	G2	0.1566	0.1441	0.1105	0.1046	0.0965	0.0862	0.0769	0.0691	0.0600	0.0585	0.0561	0.0548	0.0533	0.0465
	G3	0.1551	0.1433	0.1104	0.1046	0.0965	0.0863	0.0770	0.0692	0.0600	0.0586	0.0561	0.0549	0.0533	0.0466
	G4	0.1553	0.1434	0.1104	0.1046	0.0965	0.0863	0.0770	0.0692	0.0600	0.0586	0.0561	0.0549	0.0533	0.0465
	G5	0.1551	0.1432	0.1104	0.1046	0.0965	0.0863	0.0770	0.0692	0.0600	0.0586	0.0561	0.0549	0.0533	0.0466
	G6	0.1536	0.1424	0.1103	0.1046	0.0965	0.0863	0.0770	0.0692	0.0601	0.0586	0.0562	0.0549	0.0534	0.0466
	G7	0.1546	0.1430	0.1104	0.1046	0.0965	0.0863	0.0770	0.0692	0.0601	0.0586	0.0561	0.0549	0.0534	0.0466
	G8	0.1553	0.1433	0.1104	0.1046	0.0965	0.0863	0.0770	0.0692	0.0600	0.0585	0.0561	0.0549	0.0533	0.0465
Portland cement	Ce1	0.1666	0.1487	0.1101	0.1042	0.0960	0.0859	0.0767	0.0690	0.0599	0.0594	0.0560	0.0548	0.0533	0.0466
Cement	Ce2	0.1648	0.1472	0.1091	0.1032	0.0951	0.0851	0.0760	0.0683	0.0594	0.0579	0.0551	0.0543	0.0528	0.0462
Concrete	Ce3	0.1491	0.1394	0.1102	0.1047	0.0968	0.0869	0.0776	0.0698	0.0607	0.0592	0.0568	0.0555	0.0539	0.0471
Kapton	Po1	0.1445	0.1379	0.1119	0.1064	0.0985	0.0885	0.0791	0.0711	0.0619	0.0603	0.0578	0.0565	0.0549	0.0478
PMMA	Po2	0.1521	0.1451	0.1177	0.1120	0.1037	0.0931	0.0832	0.0748	0.0651	0.0634	0.0608	0.0594	0.0578	0.0502

polating the MAC in the range at which they remain almost unchanged is the reason for the difference between the simulated and interpolated MAC.

In addition, when comparing the interpolated MAC with experimental data [21] of the polymer materials (PMMA and Kapton), we have realized that the maximum relative deviation between them is very small at about 5.6 % (this value is 4.3 % for the simulation). This seems to be related to the type of materials. Indeed, the polymer is a large molecule with a very simple chemical composition due to multiple repeating units. Hence, a high accuracy of MAC for both the simulation and experiment could be more easily achieved. Meanwhile, the remaining materials consisting of granite, Portland cement, cement are a mixture of elements and compounds and therefore it is very difficult to precisely determine their weight and chemical composition. This caused difficulties in calculating the theoretical (NIST data) and simulated MAC, but nevertheless the experimental to interpolated MAC ratios $[(\mu/\rho)_{exp}/(\mu/\rho)_{int}]$ are mostly in the range from 0.9 to 1.1 for both groups of materials (see fig. 7).

Table 4. The calculated results of fitting parameters for 30 various materials

Group A		*a*	*b*	*c*	*d*	R^2
PbO-BaO-B2O3 glass system	P1	0.05411	–373518.6658	2.54556	0.43452	0.997
	P2	0.05305	–103058.0587	1.51816	0.44196	0.999
	P3	0.05535	–555725.6419	2.18145	0.41806	0.998
	P4	0.05349	–281823.2905	1.86657	0.43082	0.999
	P5	0.05377	–320071.5653	1.78642	0.42627	0.999
	P6	0.05381	–521605.72	2.049	0.42362	0.999
	P7	0.05612	–532252.4281	1.57967	0.40637	0.999
	P8	0.05429	–456009.8201	1.69765	0.41849	1.000
	P9	0.05418	–427470.6094	1.56429	0.41648	1.000
Gadolinium- based oxide and oxyfluoride glass systems	L1	0.0489	–42235.26454	9.85431	0.6013	0.995
	L2	0.04776	–24770.26346	11.66105	0.63888	0.995
Borate-tellurite-silicat e glass system	B1	0.05462	–364877	1.35475	0.41325	1.000
	B2	0.05602	–255615	1.00888	0.40413	1.000
	B3	0.05451	–331486	1.11167	0.40611	1.000
	B4	0.05441	–298306	0.99947	0.40342	1.000
	B5	0.05441	–310213	0.95562	0.40074	1.000
	B6	0.05424	–314257	0.91473	0.39887	1.000
Group B						
Granite	G1	–0.06357	–0.44867	0.18277	4.13108	1.000
	G2	–0.05198	–0.68008	0.8527	3.80194	1.000
	G3	–0.05935	–0.58548	0.53665	4.0235	1.000
	G4	–0.05773	–0.59957	0.57647	3.97463	1.000
	G5	–0.05965	–0.57116	0.48651	4.0311	1.000
	G6	–0.06027	–0.4167	0.13035	4.01652	1.000
	G7	–0.06147	–0.5417	0.39985	4.08431	1.000
	G8	–0.05854	–0.59245	0.55627	3.99915	1.000
Portland cement	Ce1	0.00452	–3.96103	6.61614	2.08402	0.998
Cement	Ce2	0.00323	–4.14483	7.97755	2.11055	0.998
Concrete	Ce3	–0.06045	–0.56844	0.45498	4.03376	1.000
Kapton	Po1	–0.02068	–0.2308	0.0106	2.48059	1.000
PMMA	Po2	–0.02184	–0.24298	0.01059	2.48036	1.000

CONCLUSION

With 30 investigated samples, we have succeeded in finding the mathematical function which describes the dependence of MAC *vs*. energy in the range from 100 keV to 2 MeV. The excellent agreement of the proposed function was indicated in terms of the coefficient of determination of approximately 1 for most materials. In addition, the interpolated MAC from the fitting function were also compared with the experimental and simulated data that shows good agreement. The obtained results of this work provide a different approach for evaluating the shielding properties of composite materials.

AUTHORS' CONTRIBUTIONS

The idea for this work was put forward by H. D. Tam. N. T. K. Anh and L. D. Nhat analyzed the simulated spectra using Colegram. N. T. K. Anh, L. D. Nhat and H. T. T. Ngan made the Monte Carlo input files using the MCNP5 code. The manuscript was prepared by H. D. Tam.

REFERENCES

[1] Tam, H. D., *et al*., Advanced Gamma Spectrum Processing Technique Applied to the Analysis of Scattering Spectra for Determining Material Thickness, *J Radioanal Nucl Chem., 303* (2015), 1, pp. 693-699
[2] Thanh, T. T., *et al*., Verification of Compton Scattering Spectrum of a 662 keV Photon Beam Scattered on a Cylindrical Steel Target Using MCNP5 Code, *Appl Radiat Isot., 105* (2015), Nov., pp. 294-298
[3] Nguyen, V. H., *et al*., A Semi-Empirical Method for Measuring Thickness of Pipe-Wall Using Gamma Scattering Technique, *J Radioanal Nucl Chem., 308* (2016), 3, pp. 1011-1016

Table 5. The MAC at various energies obtained from the Monte Carlo simulation

E [keV]		122	145	279	320	391	511	662	835	1115	1173	1275	1332	1408	1836
Group A		μ [cm^{2}g^{-1}]													
PbO-BaO-B_2O_3 glass system	P1	0.7572	0.4950	0.1562	0.1339	0.1095	0.0886	0.0766	0.0679	0.0581	0.0569	0.0519	0.0511	0.0505	0.0424
	P2	0.8600	0.5598	0.1677	0.1420	0.1144	0.0911	0.0779	0.0688	0.0585	0.0573	0.0523	0.0513	0.0508	0.0431
	P3	0.9634	0.6219	0.1792	0.1479	0.1193	0.0936	0.0793	0.0696	0.0589	0.0577	0.0527	0.0517	0.0511	0.0434
	P4	1.0672	0.6840	0.1907	0.1585	0.1242	0.0962	0.0807	0.0705	0.0594	0.0583	0.0531	0.0519	0.0514	0.0433
	P5	1.1722	0.7439	0.2022	0.1667	0.1291	0.0988	0.0821	0.0713	0.0598	0.0584	0.0535	0.0523	0.0516	0.0432
	P6	1.2776	0.8058	0.2137	0.1752	0.1340	0.1012	0.0835	0.0720	0.0603	0.0588	0.0538	0.0526	0.0518	0.0436
	P7	1.3844	0.8717	0.2252	0.1828	0.1389	0.1038	0.0849	0.0726	0.0606	0.0594	0.0542	0.0528	0.0522	0.0437
	P8	1.4922	0.9308	0.2367	0.1905	0.1438	0.1063	0.0863	0.0734	0.0610	0.0595	0.0546	0.0532	0.0526	0.0435
	P9	1.6015	0.9892	0.2481	0.1990	0.1487	0.1089	0.0877	0.0743	0.0615	0.0598	0.0550	0.0535	0.0527	0.0437
Gadolinium-based oxide and oxyfluoride glass systems	L1	0.3781	0.2672	0.1228	0.1141	0.0975	0.0834	0.0747	0.0671	0.0590	0.0574	0.0522	0.0516	0.0527	0.0437
	L2	0.3427	0.2465	0.1196	0.1119	0.0950	0.0828	0.0744	0.0669	0.0589	0.0573	0.0521	0.0516	0.0529	0.0440
Borate-tellurite -silicate glass system	B1	1.5694	1.0652	0.2620	0.2072	0.1504	0.1146	0.0905	0.0748	0.0613	0.0598	0.0547	0.0537	0.0526	0.0485
	B2	1.7157	1.1588	0.2780	0.2187	0.1641	0.1186	0.0923	0.0766	0.0634	0.0605	0.0549	0.0562	0.0525	0.0487
	B3	1.8661	1.2512	0.2930	0.2297	0.1677	0.1218	0.0937	0.0757	0.0626	0.0605	0.0572	0.0525	0.0531	0.0488
	B4	2.0156	1.3420	0.3101	0.2406	0.1697	0.1242	0.0954	0.0766	0.0634	0.0615	0.0561	0.0525	0.0518	0.0488
	B5	2.1630	1.4355	0.3260	0.2516	0.1799	0.1281	0.0964	0.0763	0.0633	0.0607	0.0572	0.0536	0.0538	0.0487
	B6	2.3073	1.5273	0.3418	0.2618	0.1887	0.1310	0.0978	0.0754	0.0639	0.0605	0.0572	0.0550	0.0514	0.0488
Group B															
Granite	G1	0.1399	0.1415	0.1054	0.1041	0.0938	0.0834	0.0780	0.0697	0.0611	0.0605	0.0546	0.0544	0.0538	0.0461
	G2	0.1424	0.1427	0.1055	0.1041	0.0937	0.0833	0.0779	0.0695	0.0610	0.0603	0.0545	0.0544	0.0539	0.0462
	G3	0.1411	0.1420	0.1055	0.1041	0.0937	0.0831	0.0780	0.0696	0.0606	0.0604	0.0530	0.0544	0.0539	0.0464
	G4	0.1414	0.1422	0.1055	0.1041	0.0937	0.0848	0.0780	0.0696	0.0606	0.0604	0.0533	0.0544	0.0539	0.0464
	G5	0.1413	0.1423	0.1057	0.1043	0.0939	0.0850	0.0781	0.0698	0.0608	0.0605	0.0534	0.0545	0.0540	0.0463
	G6	0.1399	0.1415	0.1054	0.1041	0.0938	0.0834	0.0780	0.0697	0.0606	0.0605	0.0546	0.0545	0.0538	0.0461
	G7	0.1407	0.1419	0.1055	0.1041	0.0938	0.0848	0.0780	0.0686	0.0606	0.0604	0.0533	0.0544	0.0538	0.0460
	G8	0.1411	0.1418	0.1055	0.1041	0.0937	0.0834	0.0780	0.0696	0.0610	0.0604	0.0546	0.0544	0.0540	0.0463
Portland cement	Ce1	0.1638	0.1473	0.1049	0.1012	0.0928	0.0866	0.0760	0.0697	0.0611	0.0611	0.0570	0.0546	0.0555	0.0479
Cement	Ce2	0.1686	0.1432	0.1057	0.0990	0.0911	0.0859	0.0772	0.0691	0.0570	0.0577	0.0565	0.0548	0.0529	0.0477
Concrete	Ce3	0.1428	0.1345	0.1057	0.1013	0.0963	0.0873	0.0765	0.0717	0.0606	0.0614	0.0574	0.0570	0.0553	0.0491
Kapton	Po1	0.1403	0.1381	0.1107	0.1074	0.0966	0.0859	0.0812	0.0720	0.0607	0.0602	0.0590	0.0570	0.0533	0.0464
PMMA	Po2	0.1495	0.1450	0.1155	0.1149	0.1068	0.0898	0.0819	0.0760	0.0644	0.0650	0.0589	0.0602	0.0554	0.0508

[4] Medhat, M. E., Application of Gamma-Ray Transmission Method for Study the Properties of Cultivated Soil, *Ann Nucl Energy, 40* (2012), 1, pp. 53-59
[5] Soane, B. D., A Gamma-Ray Transmission Method for the Measurement of Soil Density in Field Tillage Studies, *J agric Engng Res., 13* (1968), 4, pp. 340-349
[6] Alyassin, A. M., *et al*., Feasibility Study of Gamma-Ray Medical Radiography, *Appl Radiat Isot., 72* (2013), Feb., pp. 16-29
[7] Russo, P., *et al*., Combined SPECT/CT and PET/CT for Breast Imaging, *Nucl Instr Meth Phys Res A., 809* (2016), Feb., pp. 58-66
[8] Meerwaldt, R., *et al*., PET/SPECT Imaging: From Carotid Vulnerability to Brain Viability, *Eur J Radiol., 74* (2010), 1, pp. 104-109
[9] Yakalh, G., *et al*., Solid State Structural Investigations of the Bis(Chalcone) Compound with Single Crystal X-Ray Crystallography, DFT, Gamma -Ray Spectroscopy and Chemical Spectroscopy Methods, *Radiat Phys Chem., 145* (2018), Apr., pp. 89-96
[10] Dehghani, Z., *et al*., Investigation of Gamma-Ray Irradiation on Molecular Structure, Optical Properties and Mass Attenuation Coefficients of Colloidal Gold Nanoparticles, *Opt Mater, 70* (2017), Aug., pp. 99-105
[11] Gungor, A., *et al*., Flexible X/Gamma Ray Shielding Composite Material of EPDM Rubber with Bismuth Trioxide: Mechanical, Thermal Investigations and Attenuation Tests, *Prog Nucl Energy, 106* (2018), July, pp. 262-269
[12] Silva, I. L. M., *et al*., Tube Defects Inspection Technique by Using Compton Gamma-Rays Backscattering, *Nucl Instr Meth Phys Res A, 422* (1999), 1-3, pp. 957-963
[13] Xu, X., *et al*., A High Speed Compton Scatter Pipe Wall Imaging System, *Nucl Instr Meth Phys Res A., 353* (1994), 1-3, pp. 334-337
[14] Tam, H. D., Le, N. T. M., An Improved Method for Liquid Density Measurement Using NaI(Tl) Detector and Low-Strength Source, *J Radioanal Nucl Chem., 317* (2018), 1, pp. 161-168

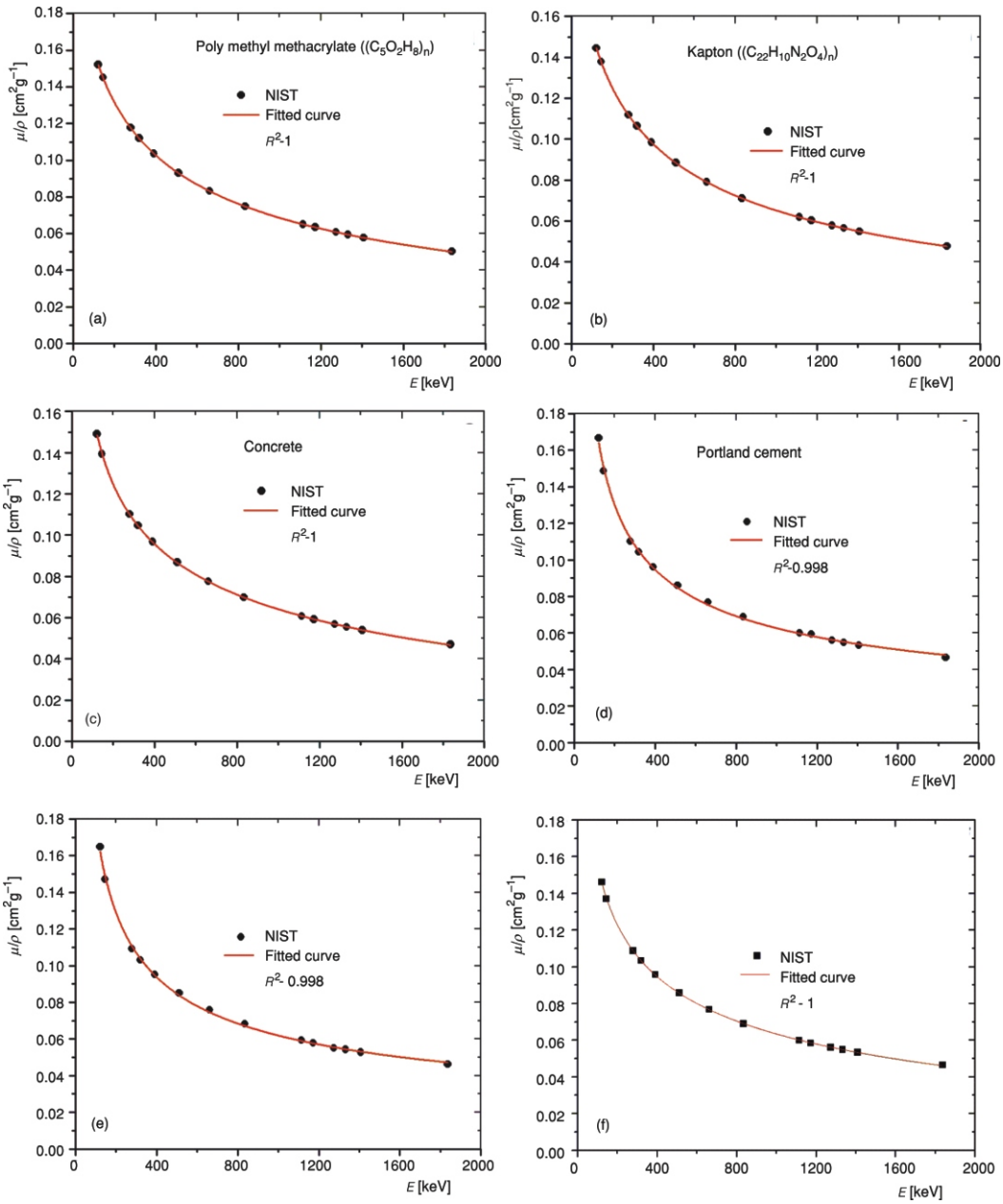

Figure 3. The energy dependence of MAC for materials of group B including PMMA (a), Kapton (b), concrete (c), Portland cement (d), cement (e), granite (f)

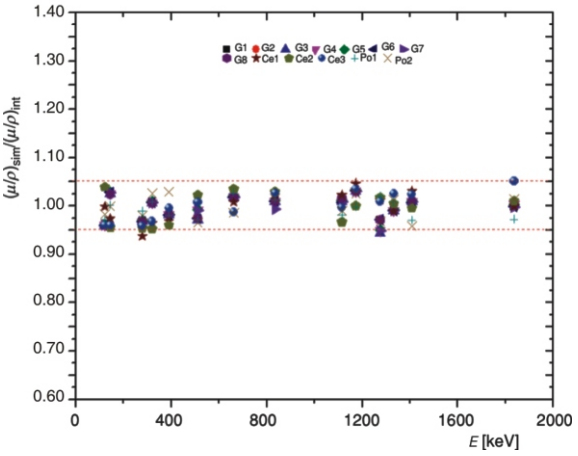

Figure 4. The simulated to interpolated MAC ratios for materials of group B

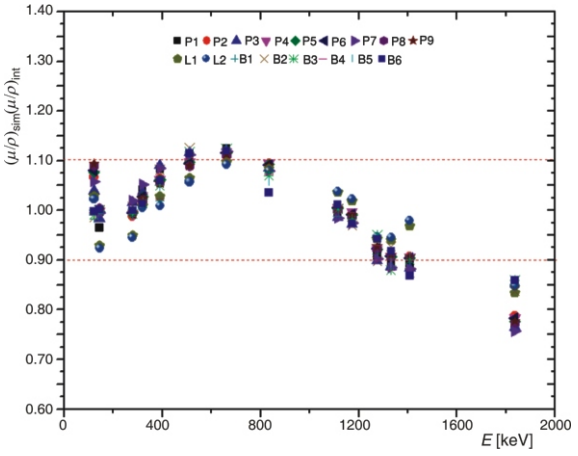

Figure 5. The simulated to interpolated MAC ratios for materials of group A

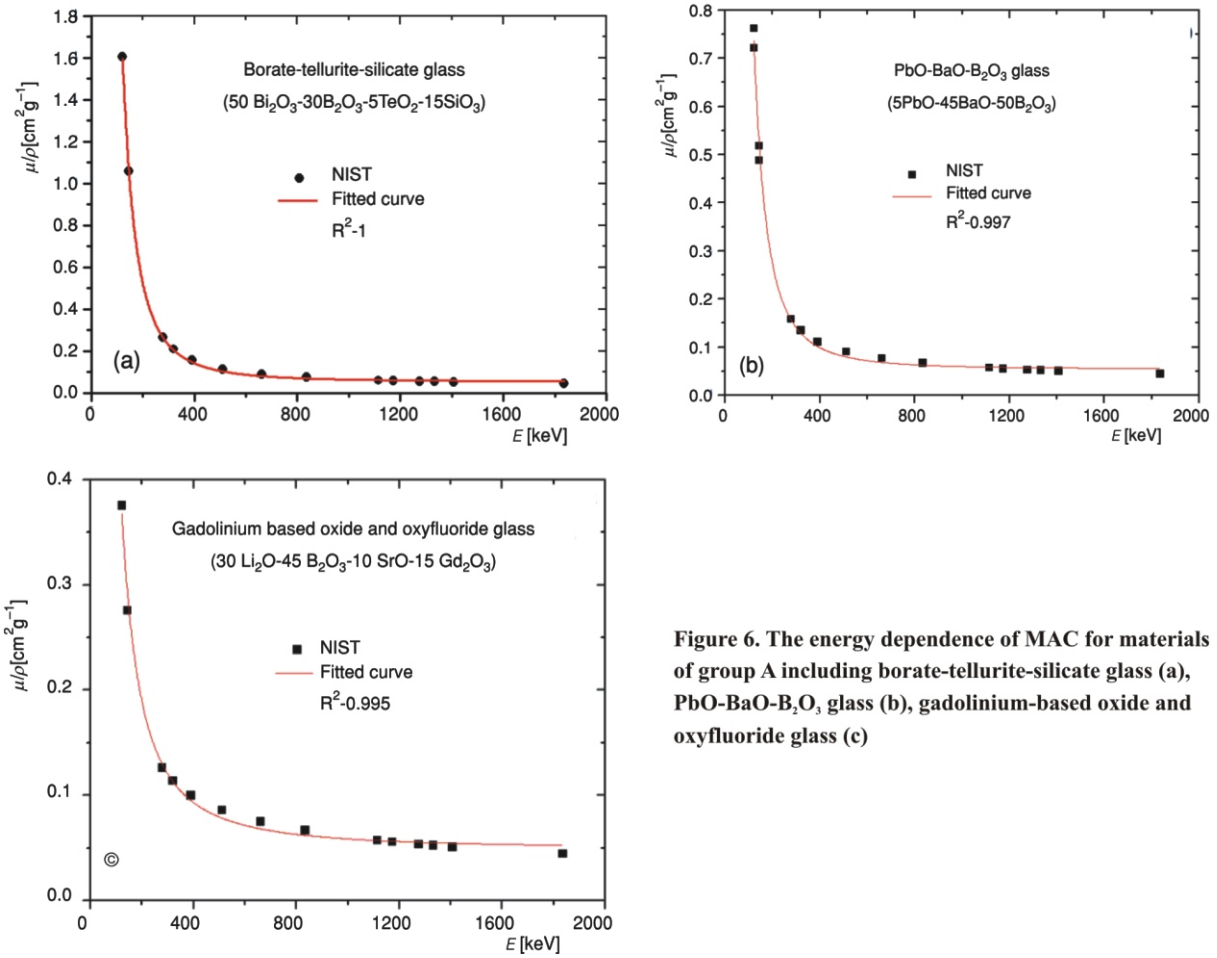

Figure 6. The energy dependence of MAC for materials of group A including borate-tellurite-silicate glass (a), PbO-BaO-B_2O_3 glass (b), gadolinium-based oxide and oxyfluoride glass (c)

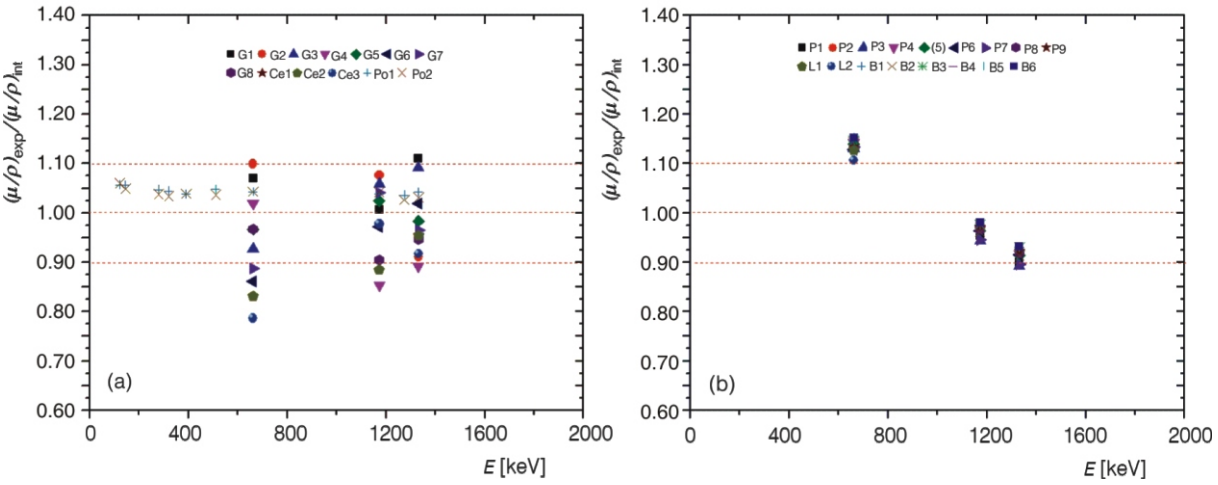

Figure 7. The experimental to interpolated MAC ratios for materials of group B (a) and group A (b)

[15] Issa, S. A. M., Effective Atomic Number and Mass Attenuation Coefficient of PbO-BaO-B_2O_3 Glass System, *Radiat Phys Chem., 120* (2016), Mar., pp. 33-37
[16] Shamshad, L., *et al*., A Comparative Study of Gadolinium Based Oxide and Oxyfluoride Glasses as Low Energy Radiation Shielding Materials, *Prog Nucl Energy, 97* (2017), May, pp. 53-59
[17] Issa, S. A. M., Mostafa, A. M. A., Effect of Bi_2O_3 in Borate-Tellurite-Silicate Glass System for Development of Gamma-Rays Shielding Materials, *J Alloys Compd, 695* (2017), Feb., pp. 302-310
[18] Kurudirek, M., *et al.*, A Study of Photon Interaction in Some Building Materials: High-Volume Admixture of Blast Furnace Slag Into Portland Cement, *Radiat Phys Chem., 78* (2009), 9, pp. 751-759
[19] Medhat, M. E., Gamma-Ray Attenuation Coefficients of Some Building Materials Available in Egypt, *Ann Nucl Energy, 36* (2009), 1, pp. 849-852
[20] Ozyurt, O., *et al*., Calculation of Gamma Ray Attenuation Coefficients of Some Granite Samples Using a Monte Carlo Simulation Code, *Radiat Phys Chem., 144* (2018), Mar., pp. 271-275

[21] Manjunatha, H. C., A Study of Gamma Attenuation Parameters in Poly Methyl Methacrylate and Kapton, *Radiat Phys Chem., 137* (2017), Aug., pp. 254-259
[22] ***, X-5 Monte Carlo team, A General Monte Carlo N-Particle Transport Code Version5, Volume II, User guide, Los Alamos National Laboratory, LA-CP-03-0245, 2005
[23] Tam, H. D., *et al*., A Study of the Effect of Al_2O_3 Reflector on Response Function of NaI(Tl) Detector, *Radiat Phys Chem., 125* (2016), Aug., pp. 88-93
[24] Tam, H. D., *et al*., Optimization of the Monte Carlo Simulation Model of NaI(Tl) Detector by Geant4 code, *Appl Radiat Isot, 130* (2017), Dec., pp. 75-79
[25] Moszynski, M., *et al.*, Temperature Depen- dences of $LaBr_3$(Ce), $LaCl_3$(Ce) and NaI(Tl) Scintillators, *Nucl Instr Meth Phys Res A, 568* (2006), 2, pp. 739-751
[26] Lepy, M. C., Presentation of the COLEGRAM Software, Note technique Laboratoire National Henri Becquerel, Gif-sur-Yvette, France, 2004
[27] ***, NIST (2010) XCOM: Photon Cross Sections Database, http://www.nist.gov/pml/data/xcom/index.cfm. Accessed 1 Nov 2017

Received on June 21, 2018
Accepted on January 17, 2019

Нгујен Ти Ким АНХ, Лам Дуј НАТ, Хо Ти Тујет НГАН, Хоанг Дук ТАМ

МАТЕМАТИЧКА ФУНКЦИЈА КОЈА ОПИСУЈЕ ЗАВИСНОСТ МАСЕНОГ АТЕНУАЦИОНОГ КОЕФИЦИЈЕНТА ОД ЕНЕРГИЈЕ КОД КОМПОЗИТНИХ МАТЕРИЈАЛА, У ЕНЕРГЕТСКОМ ОПСЕГУ ОД 100 keV ДО 2 MeV

У овом раду дат је предлог математичке функције која описује зависност масеног атенуационог коефицијента од енергије за композитне материјале у опсегу енергија од 100 keV до 2 MeV. Добијени резултати показују да предложена функција има могућност тачног описивања података са коефицијентом одлучивања R2, приближно једнаким јединици за све испитиване материјале. Користећи предложену математичку функцију, масени атенуациони коефицијенти интерполирани су, а добијене вредности упоређене са резултатима Монте Карло симулација. Поређење резултата указује на високу корелацију када је однос резултата симулација и резултата интерполације између 0.95 и 1.05. Штавише, вредности масених атенуационих коефицијената добијених интерполацијом упоређени су са експерименталним резултатима добијеним у ранијим радовима и већина односа резултата у опсегу је од 0.9 до 1.1.

Кључне речи: масени атенуациони коефицијент, Монте Карло, фитовање функције, композитни материјал